SERS and NMR Studies of Typical Aggregation-induced Emission Molecules.

ARTICLE *in* THE JOURNAL OF PHYSICAL CHEMISTRY A · JUNE 2015

Impact Factor: 2.69 · DOI: 10.1021/acs.jpca.5b05478 · Source: PubMed

THE JOURNAL OF PHYSICAL CHEMISTRY A

Article

pubs.acs.org/JPCA

SERS and NMR Studies of Typical Aggregation-Induced Emission Molecules

Cheng Fang,[†] Yujun Xie,[‡] Martin R. Johnston,[§] Yinlan Ruan,[⊥] Ben Zhong Tang,*[,#] Qian Peng,*[,‡] and Youhong Tang*[,∥]

[†]Global Centre for Environmental Remediation, University of Newcastle, Callaghan, New South Wales 2308, Australia

[‡]Key Laboratory of Organic Solids, Beijing National Laboratory for Molecular Science (BNLMS), Institute of Chemistry, Chinese Academy of Sciences, Beijing 100190, China

[§]Centre for NanoScale Science and Technology, School of Chemical and Physical Sciences, and [∥]Centre for NanoScale Science and Technology, School of Computer Science, Engineering and Mathematics, Flinders University, Bedford Park, South Australia 5042, Australia

[⊥]Institute of Photonics and Advanced Sensing, School of Physical Science, The University of Adelaide, Adelaide 5005, Australia

[#]Department of Chemistry, The Hong Kong University of Science and Technology, Hong Kong, China

Supporting Information

ABSTRACT: Over recent decades, aggregation-induced emission (AIE) molecules have attracted increasing attention. Restriction of intramolecular rotation (RIR) has been widely accepted as the cause of the emission when AIE molecules aggregate into clusters. The intramolecular rotation of AIE molecules can be monitored by molecular vibration spectra such as nuclear magnetic resonance (NMR), infrared, and Raman, especially surface-enhanced Raman scattering (SERS) which has high sensitivity down to a single molecule. We employed SERS and NMR to study the AIE emission mechanism and compared experimental results with simulation data to monitor the RIR. Interestingly, we found that intramolecular rotation was also restricted for individual AIE molecules loaded onto SERS substrate surfaces due to the laid-down configuration.

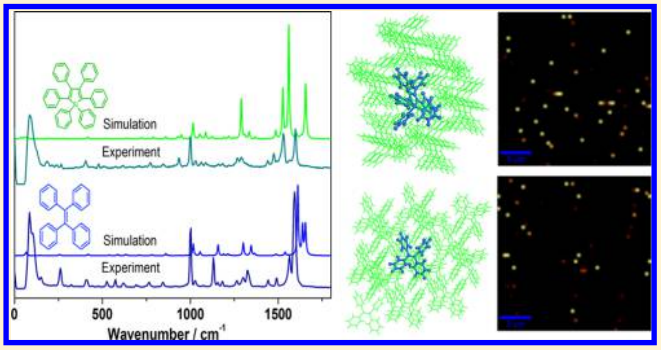

1. INTRODUCTION

Around half a century ago, Förster and Kasper discovered that the fluorescence of pyrene weakened with an increase in its solution concentration.[1] It was soon recognized that this was a general phenomenon for many aromatic compounds. This concentration-quenching effect was found to be caused by the formation of sandwich-shaped excimers and exciplexes aided by the collisional interactions between the aromatic molecules in the excited and ground states, which "are now known to be common to most aromatic hydrocarbons and their derivatives", as summarized by Birks in 1970 in his classic book *Photophysics of Aromatic Molecules*.[2]

In 2001 we discovered such a system,[3−6] in which luminogen aggregation played a constructive rather than destructive role in the light-emitting process: a series of silole molecules were found to be nonluminescent in the solution state but emissive in the aggregated state (as nanoparticle suspensions in poor solvents or as thin films in the solid state). We coined the term "aggregation-induced emission" (AIE) for this novel phenomenon because the nonluminescent silole molecules were induced to emit by aggregate formation.

We hypothesized that restriction of the intramolecular rotation (RIR) process is the main cause of the AIE effect.[3−6] To check the validity of this hypothesis, we performed a series of tests to externally and internally modulate the RIR process. In solution, the multiple aryl blades of the silole molecules rotate around the single-bond axles linking the peripheral aryl rotors and the central stator of the silacyclopentadiene core. This intramolecular rotation converts photonic energy to heat and deactivates the excited states nonradiatively, thus making the molecules nonemissive. In aggregates, the intramolecular rotation is restricted and the nonradiative relaxation channel is obstructed. Thanks to their propeller-like shapes, the silole molecules experience little $\pi-\pi$ stacking interaction in the condensed phase and thus have little opportunity to form excimer species. The activated RIR process and the reduced likelihood of excimer formation together make the silole molecules highly emissive in the solid state.

Received: April 1, 2015
Revised: June 23, 2015

DOI: 10.1021/acs.jpca.5b05478
J. Phys. Chem. A XXXX, XXX, XXX−XXX

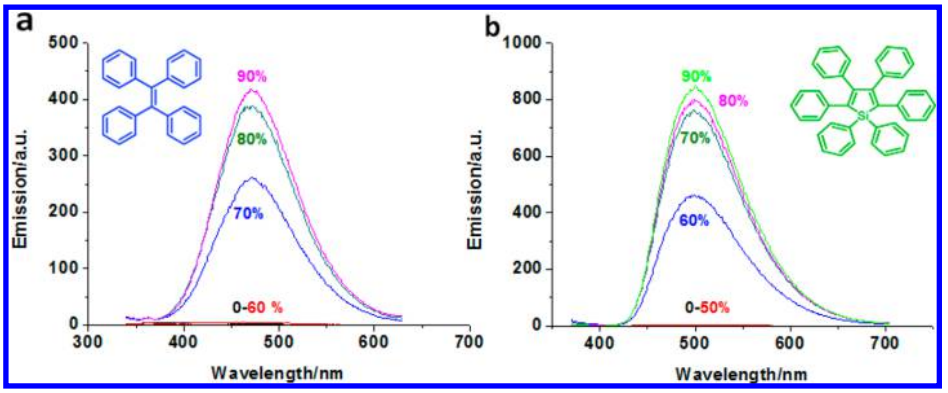

Figure 1. Fluorescence spectra of TPE (a) and HPS (b) depending on the fraction of water in acetone solution. TPE and HPS concentrations were both 10 μM. Insets show the molecular structure of tetraphenylethene (TPE, left) and hexaphenylsilole (HPS, right).

RIR can be directly confirmed by redesigning the molecular structure and quantitatively theoretical calculations and analyses.[7−9] More directly, if the silole molecules are emissive, in which fluorescence is usually observed, other spectroscopic techniques should also provide similar information such as Raman scattering which commonly competes with fluorescence emission because they have similar origins.[10] As an alternative, surface-enhanced Raman scattering (SERS) is a spectroscopic technique that provides a greatly enhanced Raman signal from Raman-active analyte molecules that have been adsorbed onto certain specially prepared metal surfaces.[10−13] Increases in the intensity of Raman signal have been regularly observed in the order of 10^4−10^6 and can be as high as 10^8 and 10^{14} for some systems.[14,15] SERS selectivity of surface signal results from the presence of surface enhancement mechanisms only at the surface. Thus, the surface signal overwhelms the bulk signal, making bulk subtraction unnecessary.

Nanoroughened or nanoporous silver surfaces have been used as SERS substrates.[10] More recently, electrochemical roughening has been used to further optimize surface-enhanced Raman effects, even allowing single molecule detection when pore etching occurs.[16−18] The ordered nanostructure is also receiving increasing attention. Nanostructure substrate fabrication usually involves lithography, including nanosphere,[19] photomask,[20] e-beam,[10] or self-assembly.[17,21] To further boost the enhancement, SERS dual substrates have recently been developed.[15,22−24] Taking the substrate of a pore array as an example,[20,25] the idea is to fill the pores with nanoparticles. In consequence, the morphology of the dual substrate combines the primarily enhanced electromagnetic field from the pore array with the subsequently enhanced electromagnetic field arising from the nanoparticles. In this research, we employed SERS to differentiate AIE molecules in aggregated and dissolved states on a SERS dual substrate and to illustrate the AIE mechanism in another way. We also *in situ* monitored the aggregation process via observing the modification of the Raman spectra that originated from molecular vibration. Raman simulation was performed to visualize the AIE molecule conformations on the Ag surface in aggregated and dissolved states. On the other hand, NMR also provides the direct information about the RIR process so that we also used the simulated and experimental NMR data to identify the RIR of AIE in solution and in cluster.

2. EXPERIMENTAL SECTION

2.1. Materials. All chemicals, namely acetone, hexane, and silver colloid (AgNP), were purchased from Sigma-Aldrich (Australia). They were used directly without further purification. Milli-Q water (~18 MΩ) was used for washing and dilution.

Here we examine two typical AIE luminogens: tetraphenylethene (TPE) and hexaphenylsilole (HPS). They are synthesized according to the literature,[26,27] and their structure is shown in Figure 1 (insets). When AIE molecules are dissolved as isolated species in solution, less restriction is imposed on their intramolecular rotation. The intramolecular rotation of phenyl rings in the AIE molecules may induce an efficient nonradiative annihilation process, such that the AIE solution is nearly nonemissive. On the other hand, if the rotation of phenyl rings in the AIE molecule is restricted, emission of the molecule may be turned on due to blocking of the nonradiative annihilation process.

2.2. Preparation of Dual Substrate. A pore array of SERS substrate has been reported previously[20] and fabricated in the Institute of Microelectronics (IME), A-Star, Singapore. Silver colloid with a diameter of ~10 nm was purchased for fabrication of the dual substrate. In general, ~10 μL of silver colloid solution was dropped onto the pore array surface and dried in air at room temperature. It was washed with Milli-Q water before use.

AIE was loaded onto the dual-substrate surface either by incubating the dual substrate in solution or by dropping ~5 μL of solution and drying in air. Before testing, the surface was washed with Milli-Q water.

2.3. Characterizations. The photoluminescence (PL) spectra of the silole solutions and the nanoaggregate mixtures were recorded on a Cary Eclipse fluorescence spectrophotometer (Agilent Technologies, USA). Scanning electron microscopy (SEM) (Quanta 450, FEI Co., USA) was used to characterize the surface topography of the dual substrate.

All SERS spectra were collected in air using a Witec Confocal Raman microscope (Witec, Germany) equipped with a 532 nm laser diode (<60 mW). A CCD detector (cooled at ~−60 °C) was used to collect Stokes Raman signals at room temperature (~24 °C) in the wavenumber range of 400−2000 cm^{-1} with an exposure time slot of 5 s for each measurement. In a typical experiment, several spectra were recorded for each substrate at several randomly selected laser spots, in order to characterize possible nonuniform distribution. We observed the similar spectra without peak position variation but with peak intensity

DOI: 10.1021/acs.jpca.5b05478
J. Phys. Chem. A XXXX, XXX, XXX−XXX

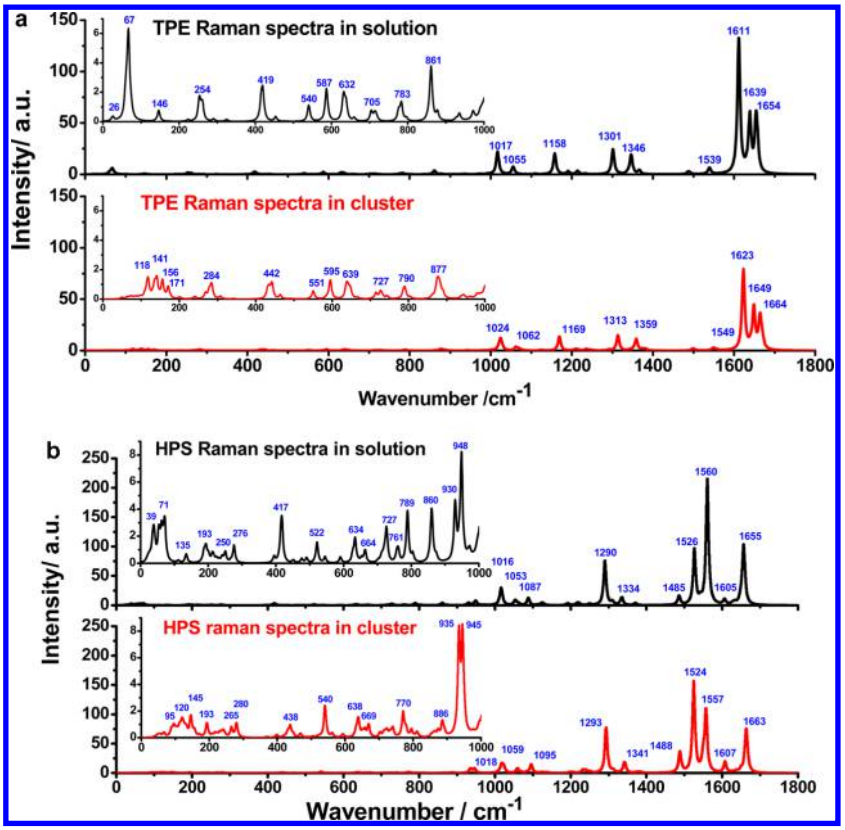

Figure 2. Calculated Raman spectra of TPE (a) and HPS (b). Insets show the zoomed-in area at the low wavenumber ranges.

variation (<30%). Usually, the typical spectra (average one from the measured area) were shown.

For the mapping of AIE under Raman microscopy, the excitation laser was scanned over the dual-substrate surface over an area of 25 μm × 25 μm with a pixel array of 50 × 50 while the Raman signal was collected with an integration time of 0.1 s for each pixel. The mapping image was generated based on the intensity of the characteristic Raman peaks of the AIEs. For time series Raman, a drop of solution was distributed on the dual-substrate surface (~5 mm × 5 mm). The solvent was vaporized in air gradually while the Raman signals were collected every second with an integration time of 0.5 s and duration of 100 s.

^{13}C NMR spectra were recorded in deuterated chloroform ($CDCl_3$) and referenced to a residual solvent signal. Chemical shifts are reported as parts per million (ppm). ^{13}C solid state cross-polarization magic-angle spinning nuclear magnetic resonance (13C CP/MAS NMR) measurements were performed on a Bruker Avance III 400 MHz spectrometer equipped with a 7 mm solid state probe. The sample was spun at 2.5 kHz; CP/MAS was carried out with a 2 ms mixing time that was varied according to the ramp Bruker program. The spectral width was 250 ppm, acquisition time 30 ms, and recycle delay 5 s.

2.4. Computational Methods. The molecular geometry optimizations and Raman spectra were performed at the level of B3LYP/6-31G(d). The solvent effect is modeled by adopting the polarizable continuum model (PCM). The aggregation effect is mimicked through cutting a large cluster from the X-ray diffractions crystal structure by using quantum mechanics coupled with molecular mechanics (QM/MM) with two-layer ONIOM method. The NMR chemical shifts were calculated by using the GIAO method at the same level. C and H relative chemical shifts (δ) were obtained in reference to those of tetramethylsilane (TMS). All the calculations were carried out by using Gaussian 09 program;[28] see the Supporting Information for more details.

3. RESULTS AND DISCUSSION

3.1. Photoluminescence. PL spectra of HPS and TPE in aggregated and dissolved states are presented in Figure 1. Strong emission was observed when the fraction of water increased to 75% for the TPE and 60% for the HPS. It has been confirmed that the aggregation of AIE occurs when its solubility in acetone−water decreases with the increasing fraction of water.[5,6] Restriction of intramolecular rotation is responsible for the emission.[9,29]

3.2. Simulated and Experimental Raman Spectra. Figure 2 shows the simulated Raman spectra of TPE and HPS, and Figures S2 and S3 give the detailed assignment of the Raman-active normal vibration modes. The main changes appear in the low-frequency vibrational normal modes for TPE and HPS from in solution to cluster. There are so large blue-shifts for the low-frequency vibrational normal modes that the ones less than 100 cm^{-1} disappear in solid state compared to solution. This is easily understood because the low-frequency modes are assigned as the rotation motions of the peripheral flexible phenyl rings from Figures S2 and S3, which are easily affected by the surrounding environments. In solid state, the intramolecular rotation motions are efficiently restricted by the intermolecular interaction between the surrounding molecules. The potential energies caused by the normal modes are improved, which resulted in the blue-shift of the peaks. The higher frequency vibrational motions with Raman-active are

DOI: 10.1021/acs.jpca.5b05478
J. Phys. Chem. A XXXX, XXX, XXX−XXX

mostly ascribed to the mixed breathing vibrations or stretching vibrations in plane and vibrations out of plane, which are slightly affected by the surrounding environment and exhibit a little blue-shift from solution to solid state. The other Raman-active modes belong to pure inner bending or breathing or stretching vibrations in plane, which are hardly impacted by the intermolecular interaction, and there are no blue-shifts from in solution to solid state, namely some modes for HPS as seen in Figure 2b.

In order to characterize the restriction of the intramolecular rotation, we further calculated the rotational energy barriers of the phenyl groups at site 1 of ethylene for TPE and site 2 of silacycle for HPS in solution and cluster in Figures 3a and 3b,

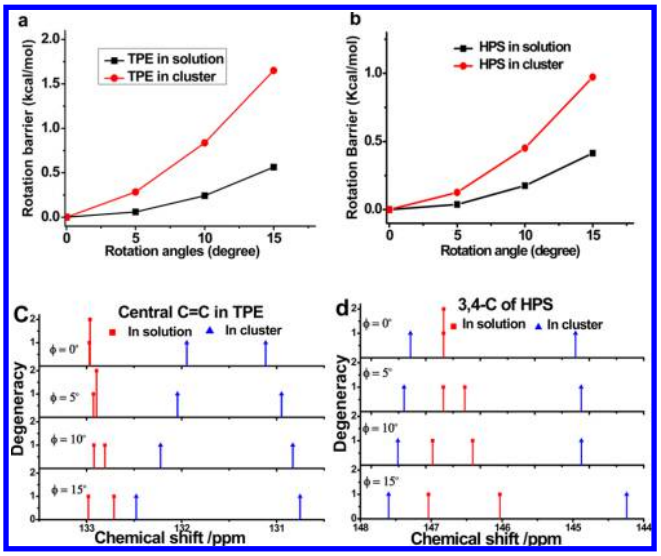

Figure 3. Calculated rotational energy barrier (a, b) and C NMR (c, d) at site 1 and 2 of TPE and at site 2 and 3 of silacycle for HPS in solution and cluster as a function of rotational angle ϕ of phenyl ring at site 1 of ethylene for TPE and at site 2 of silacycle for HPS.

respectively. The results clearly indicate that the phenyl rings can rotate much easier in solution than those in solid state for both TPE and HPS. In addition, the nuclear magnetic resonance (NMR) is also a good technique to verify the restricted intramolecular motion because the changes in the signal can be unambiguously attributed to molecular mobility.[30−32] Hence, we examined the rotation-induced conformation changes by rotating a phenyl ring upon a single-bond axis, and the calculated results are shown in Figures 3c and 3d. The rotation of the phenyl ring causes a much larger splitting value in solution than that in cluster. This thus confirms that the intramolecular rotations are indeed restricted in the solid state. The experimental data of NMR are listed in Figure S4.

3.3. Aggregate vs Individual AIEs (TPE and HPS). In Figure 4a, the collected Raman spectra from the dried SERS substrate surface are compared with the simulated spectra (cluster). In general, they match well except for some shifts of peak position and variation of peak intensity, which are acceptable when considering the ideal situation for simulation, such as a single molecule from a bulk crystal. Figure 4b shows the surface morphology of the dual substrate.[25] The AgNPs were aggregated from the initial size of ∼10 to ∼100 nm when the colloid was dried on the pore array surface. The inset shows that most of the Ag particles are localized within the pore, the structure of which has been reported by us previously.[20]

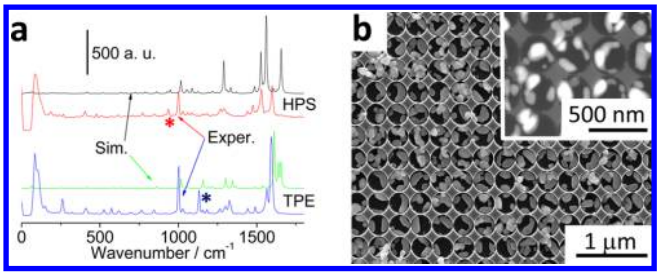

Figure 4. Raman spectra of AIE (a) and SERS substrate (b) used for Raman signal collection. (a) shows the experimental spectra (SERS) of AIE while the simulated spectra (in cluster) are also presented for comparison. The AIE solution of 1×10^{-4} M in acetone was dropped (∼10 μL) onto the SERS substrate surface for drying in air.

In Figure 5, the limit of detection (signal-to-noise ratio >3) was estimated to be $\sim 5 \times 10^{-6}$ M for TPE and $\sim 5 \times 10^{-7}$ M

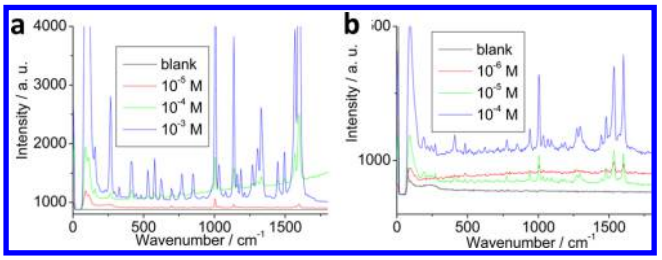

Figure 5. SERS spectra depending on concentration of AIEs: TPE (a); HPS (b) in acetone. All the spectra were collected from the dried SERS substrate surface. For more information please refer to Figure 2.

for HPS. The lower value of HPS is due to the larger molecular cross section of HPS than that of TPE, if we ignore the difference between their loading affinities. No peak shift was observed when the concentration was diluted for 1000 times. At the high concentration, most of the AIE molecules were aggregated when the dual substrate was dried. Therefore, the Raman signal originates from the aggregate configuration, in which the intramolecular rotation has been restricted. At low concentration, the aggregate was not the dominant configuration, rather the individual molecule. However, those individual AIE molecules featured a similar Raman signal, suggesting there was also no free rotation. The adsorbed AIE molecule was most likely laid down on the Ag surface or is planarized to the surface. As consequence, the rotation of the benzyl group was also restricted.[3,4]

To confirm that the Raman spectra collected from the low concentration of AIE originated from the individual molecule, we carried out a bianalyte analysis. Figure 6 shows the mapping

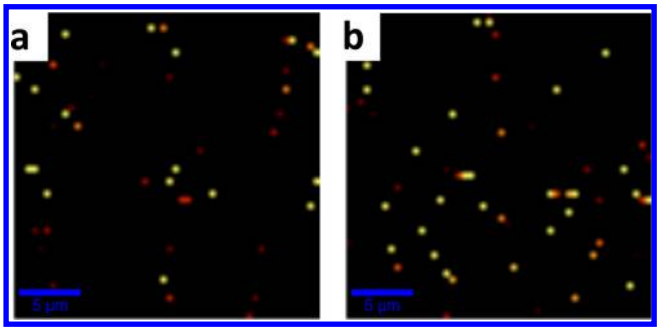

Figure 6. Raman mapping images of TPE (a) and HPS (b).

DOI: 10.1021/acs.jpca.5b05478
J. Phys. Chem. A XXXX, XXX, XXX−XXX

images of TPE at 10^{-5} M and HPS at 10^{-6} M. The characteristic peaks for mapping are shown in Figure 4a (experiment, marked by stars). The overlapping is <5%, indicating that single molecule detection of TPE/HPS (41/49 in number) has been attained.[17−19] Note the number was estimated from the bright spots in Figure 6, which was related with the nanostructure on the surface (Figure 4b), loading affinity, Raman activity, etc. Even for those spectra from single molecule, we did not observe the peak shifting when compared to the aggregate configuration at the high concentration (as shown in Figure 5). Because the high concentration leaded to the AIE molecules to aggregate into cluster and RIR, the similar Raman spectra of those single AIE molecules with the cluster suggested their molecular configuration and environment were the same. In other words, single AIE molecule also experienced the RIR, indicating the laid-down configuration of the individual AIE molecule on the dried SERS surface. As a consequence, we found that the laid-down (planarized on the surface) individual AIE features a Raman spectrum similar to that of the aggregate AIE (high concentration).

To further identify the aggregate configuration of AIE on the dried dual-substrate surface, the different loading approaches of AIE were compared, as shown in Figure 7. In the "drop and dry" approach, the AIE molecules were aggregated when the solvent vaporized, leading to the increased concentration of AIE in the residual solution. Furthermore, the vaporization speed of acetone is much faster than that of water, which means that the fraction of water is also increased during vaporization. As a consequence, the loaded moieties are dominated by the aggregated AIE, as evidenced by the strong background in Figures 7a and 7c, which represent the fluorescence.

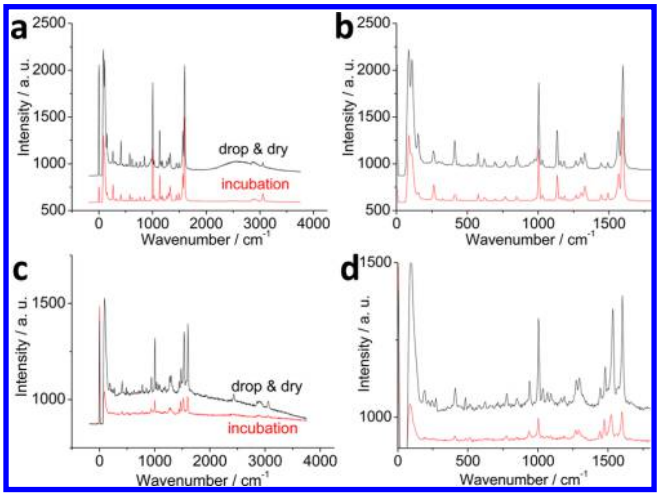

Figure 7. Comparison of the different loading approaches of AIE: spectra of TPE under different magnifications (a, b); spectra of HPS (c, d). "Drop and dry" means that ~2 μL solution of 0.1 mM AIE acetone/water (1:1, v/v) was dropped onto the SERS substrate surface and dried in air. "Incubation" means that the SERS substrate was immersed in a solution of 0.1 mM AIE acetone (100%) overnight and then washed.

It was known that the AIE molecules were free individual molecules in pure acetone (100%) solution, so that the loading moieties should be individual AIE molecules from the incubation process. However, again, we did not see obvious differences between them, whether for TPE in Figures 7a and 7b or for HPS in Figures 7c and 7d, confirming our above assumption that the individual AIE molecule was laid down on the SERS substrate surface with the result that free intramolecular rotations were restricted.

3.4. *In Situ* Observation from Free AIEs to Aggregated AIEs. Figure 8 shows the time-series Raman signals for *in situ* monitoring of the aggregation process from individual AIE molecules. The AIE was dissolved in acetone (100%) at 1×10^{-3} M. A drop of the solution (~0.1 mL) was localized on dual SERS substrate surface, and the time-dependent Raman spectra were collected while the acetone gradually vaporized. Note that the Raman signal of the acetone has been removed for clarity. In both cases of TPE in Figure 8a and HPS in Figure 8b, we observed a positive shift of the main peaks when the solvent was vaporized, suggesting the aggregation process of the AIE, which is in good agreement with the simulation results (Figures S1−S3).

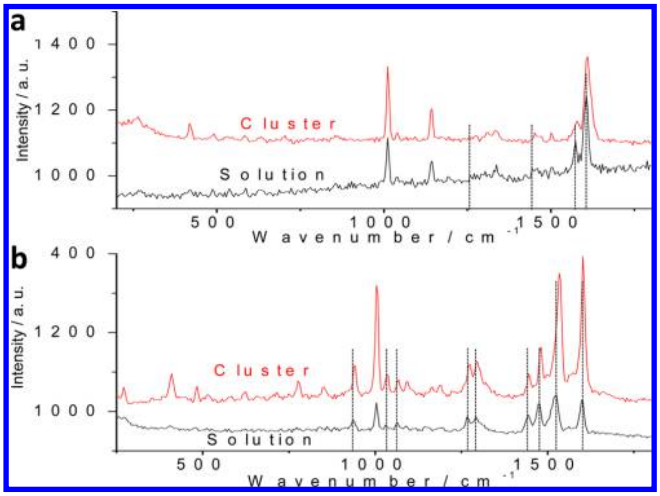

Figure 8. Raman spectra of TPE (a) and HPS (b) are dependent on their molecular configuration. Both TPE and HPS of 1 mM were dissolved in acetone (100%). The spectra were typical at the beginning (solution) and end (cluster after vaporisation) of a time-series Raman.

4. CONCLUSION

We simulated the Raman and NMR spectra of two typical AIEs: TPE and HPS. We compared the simulation data with experimental results and confirmed the hypothesis that the photoluminescence mechanism of AIE is attributable to the restricted intramolecular rotations. We also noted that individual AIE molecules featured restriction of intramolecular rotations on the metal surface (here, silver for the SERS substrate), most likely due to the laid-down configuration of the AIE molecules.

■ ASSOCIATED CONTENT

Supporting Information

Molecular geometry optimizations; each peak of simulated Raman spectra; calculated and experimental solid and liquid NMR spectra of carbon atom for HPS and TPE in solution and cluster. The Supporting Information is available free of charge on the ACS Publications website at DOI: 10.1021/acs.jpca.5b05478.

■ AUTHOR INFORMATION

Corresponding Authors

*Tel 852-23587375, e-mail tangbenz@ust.hk (B.Z.T.).

DOI: 10.1021/acs.jpca.5b05478
J. Phys. Chem. A XXXX, XXX, XXX−XXX

*Tel 86-10-62554001, e-mail qpeng@iccas.ac.cn (Q.P.).
*Tel 61-8-82012138, e-mail youhong.tang@flinders.edu.au (Y.T.).

Author Contributions

C.F. and Y.X. made equal contributions.

Notes

The authors declare no competing financial interest.

REFERENCES

(1) Förster, Th.; Kasper, K. Ein Konzentrationsumschlag der Fluoreszenz. *Z. Phys. Chem. (Munich)* **1954**, *1*, 275−277.
(2) Birks, J. B. *Photophysics of Aromatic Molecules*; Wiley: London, 1970.
(3) Ding, D.; Li, K.; Liu, B.; Tang, B. Z. Bioprobes Based on AIE Flurogens. *Acc. Chem. Res.* **2013**, *46*, 2441−2453.
(4) Mei, J.; Hong, Y.; Lam, J. W. Y.; Qin, A.; Tang, Y.; Tang, B. Z. The Whole is More Brilliant Than the Parts. *Adv. Mater.* **2014**, *26*, 5429−5479.
(5) Li, Z.; Dong, Y.; Mi, B.; Tang, Y.; Häussler, M.; Tong, H.; Dong, Y.; Lam, J. W. Y.; Ren, Y.; Sung, H. H. Y.; et al. Structural Control of the Photoluminescence of Silole Regioisomers and Their Utility as Sensitive Regiodiscriminating Chemosensors and Efficient Electroluminescent Materials. *J. Phys. Chem. B* **2005**, *109*, 10061−10066.
(6) Zeng, Q.; Li, Z.; Dong, Y.; Di, C.; Qin, A.; Hong, Y.; Ji, L.; Zhu, Z.; Jim, C. K. W.; Yu, G.; et al. Fluorescence Enhancements of Benzene-Cored Luminophors by Restricted Intramolecular Rotations: AIE and AIEE Effects. *Chem. Commun.* **2007**, 70−72.
(7) Peng, Q.; Yi, Y. P.; Shuai, Z. G.; Shao, J. S. Toward Quantitative Prediction of Molecular Fluorescence Quantum Efficiency: Role of Duschinsky Rotation. *J. Am. Chem. Soc.* **2007**, *129*, 9333−9339.
(8) Wu, Q. Y.; Deng, C. M.; Peng, Q.; Niu, Y. L.; Shuai, Z. G. Quantum Chemical Insights into the Aggregation Induced Emission Phenomena: A QM/MM Study for Pyrazine Derivatives. *J. Comput. Chem.* **2012**, *33*, 1862−1869.
(9) Zhang, T.; Jiang, Y. Q.; Niu, Y. L.; Peng, Q.; Shuai, Z. G. Aggregation Effects on the Optical Emission of 1,1,2,3,4,5-hexaphenylsilole (HPS): A QM/MM Study. *J. Phys. Chem. A* **2014**, *118*, 9094−9104.
(10) Haynes, C. L.; McFarland, A. D.; Duyne, R. P. V. Surface-enhanced Raman Spectroscopy. *Anal. Chem.* **2005**, *77*, 338A−346A.
(11) Mortazavi, D.; Kouzani, A. Z.; Kaynak, A.; Duan, W. In *Proceeding of the IEEE/ICME International Conference on Complex Medical Engineering*; IEEE: China, 2011.
(12) Rycenga, M.; Cobley, C. M.; Zeng, J.; Li, W.; Horan, C. H.; Zhang, Q.; Qin, D.; Xia, Y. Controlling the Synthesis and Assembly of Silver Nanostructures for Plasmonic Applications. *Chem. Rev.* **2011**, *111*, 3669−3712.
(13) Stiles, P. L.; Dieringer, J. A.; Shah, N. C.; van Duyne, R. P. Surface-Enhanced Raman Spectroscopy. *Annu. Rev. Anal. Chem.* **2008**, *1*, 601−626.
(14) Halvorson, R. A.; Vikesland, J. Surface-enhanced Raman Spectroscopy (SERS) for Environmental Analyses. *Environ. Sci. Technol.* **2010**, *44*, 7749−7755.
(15) Tong, L.; Zhu, T.; Liu, Z. Approaching the Electromagnetic Mechanism of Surface-enhanced Raman Scattering: from Self-assembled Arrays to Individual Gold Nanoparticles. *Chem. Soc. Rev.* **2011**, *40*, 1296−1304.
(16) Fang, C.; Agarwal, A.; Widjala, E.; Garland, M. V.; Wong, S. M.; Linn, L.; Khalid, N. M.; Salim, S. M.; Balasubramanian, N. Metallization of Silicon Nanowires and SERS Response from a Single Metallized Nanowire. *Chem. Mater.* **2009**, *21*, 3542−3548.
(17) Fang, C.; Brodoceanu, D.; Kraus, T.; Voelcker, N. H. Templated Silver Nanocube Arrays for Single-molecule SERS Detection. *RSC Adv.* **2013**, *3*, 4288−4293.
(18) Fang, C.; Ellis, A. V.; Voelcker, N. H. Electrochemical Synthesis of Silver Oxide Nanowires, Microplatelets and Application as SERS Substrate Precursors. *Electrochim. Acta* **2012**, *59*, 346−353.
(19) Fang, C.; Bandaru, N. M.; Voelcker, N. H. Beta-cyclodextrin Decorated Nanostructured SERS Substrates Facilitate Selective Detection of Endocrine Disruptor Chemicals. *Biosens. Bioelectron.* **2013**, *42*, 632−639.
(20) Fang, C.; Agarwal, A.; Buddharaju, K. D.; Khalid, N. M.; Salim, S. M.; Widjaja, E.; Garland, M. V.; Balasubramanian, N.; Kwong, D. L. DNA Detection Using Nanostructured SERS Substrates with Rhodamine B as Raman Label. *Biosens. Bioelectron.* **2008**, *24*, 216−221.
(21) Brodoceanu, D.; Fang, C.; Voelcker, N. H.; Bauer, C. T.; Wonn, A.; Arzt, E.; Kraus, T. Fabrication of Metal Nanoparticle Arrays by Controlled Decomposition of Polymer Particles. *Nanotechnology* **2013**, *24*, 085304.
(22) Jiao, Y.; Dmitry, S. K.; Phambu, N.; Weiss, S. M. Controlling Surface Enhanced Raman Scattering Using Grating-type Patterned Nanoporous Gold Substrates. *Appl. Phys. Lett.* **2010**, *97*, 153125.
(23) Leverette, C. L.; Shubert, V. A.; Wade, T. L.; Varazo, K.; Dluhy, R. A. Development of A Novel Dual-layer Thick Ag Substrate for Surface-enhanced Raman Scattering (SERS) of Self-assembled Monolayers. *J. Phys. Chem. B* **2002**, *106*, 8747−8755.
(24) Li, H.; Cullum, B. M. Dual Layer and Multilayer Enhancements from Silver Film over Nanostructured Surface-enhanced Raman Substrates. *Appl. Spectrosc.* **2005**, *59*, 410−417.
(25) Ahn, H. J.; Thiyagarajan, P.; Jia, L.; Kim, S. I.; Yoon, J. C.; Thomas, E. L.; Jang, J. H. An Optimal Substrate Design for SERS: Dual-scale Diamond-shaped Gold Nano-structures Fabricated via Interference Lithography. *Nanoscale* **2013**, *5*, 1836−1842.
(26) Hong, Y.; Lam, J. W. Y.; Tang, B. Z. Aggregation-induced Emission: Phenomenon, Mechanism and Applications. *Chem. Commun.* **2009**, 4332−4353.
(27) Chen, J.; Law, C. C. W.; Lam, J. W. Y.; Dong, Y.; Lo, S. M. F.; Williams, I. D.; Zhu, D.; Tang, B. Z. Synthesis, Light Emission, Nanoaggregation, and Restricted Intramolecular Rotation of 1,1-substituted 2,3,4,5-tetraphenylsiloles. *Chem. Mater.* **2003**, *15*, 1535−1546.
(28) Frisch, M. J.; Trucks, G. W.; Schlegel, H. B.; Scuseria, G. E.; Robb, M. A.; Cheeseman, J. R.; Scalmani, G.; Barone, V.; Mennucci, B.; Petersson, G. A. *Gaussian 09, Revision D.01*; Gaussian, Inc.: Wallingford, CT, 2013.
(29) Leung, N. L. C.; Xie, N.; Yuan, W. Z.; Liu, Y.; Wu, Q. Y.; Peng, Q.; Miao, Q.; Lam, J. W. Y.; Tang, B. Z. Restriction of Intramolecular Motions: The General Mechanism Behind Aggregation-induced Emission. *Chem.—Eur. J.* **2014**, *20*, 15349−15353.
(30) Yuan, X.; Sperger, D.; Munson, E. J. Investigating Miscibility and Molecular Mobility of Nifedipine-PVP Amorphous Solid Dispersions Using Solid-state NMR Spectroscopy. *Mol. Pharmaceutics* **2014**, *11*, 329−337.
(31) Lemaster, C. B. NMR Spectroscopy of Molecules in the Gas Phase. *Prog. Nucl. Magn. Reson. Spectrosc.* **1997**, *31*, 119−154.
(32) Hofman, S.; Gao, L.; van Dingenen, H.; Hosten, N. G. C.; van Haver, D.; De Clercq, P. J.; Milanesil, M.; Viterbo, D. A Short Intramolecular Diels-alder Route to Himbacine Derivatives. *Eur. J. Org. Chem.* **2001**, *15*, 2851−2860.

DOI: 10.1021/acs.jpca.5b05478
J. Phys. Chem. A XXXX, XXX, XXX−XXX